ELSEVIER

International Journal of Mass Spectrometry 185/186/187 (1999) 745–757

International Journal of Mass Spectrometry

Carbyne thermochemistry from energy-resolved collision-induced dissociation. The heats of formation of CH, CF, and CCl

Rachel A. Jesinger, Robert R. Squires*

Department of Chemistry, Purdue University, West Lafayette, IN 47907, USA

Received 9 July 1998; accepted 8 September 1998

Abstract

The 298 K heats of formation of the carbynes CH, CF, and CCl have been determined from measurements of the chloride dissociation energies of the halocarbene anions, $CHCl^{\cdot -}$, $CFCl^{\cdot -}$, and $CCl_2^{\cdot -}$. The chloride dissociation enthalpies were measured by energy-resolved collision-induced dissociation in a flowing afterglow—triple quadrupole instrument to be 37.7 ± 2.3, 21.9 ± 1.1, and 33.4 ± 2.3 kcal/mol, for $CHCl^{\cdot -}$, $CFCl^{\cdot -}$, and $CCl_2^{\cdot -}$, respectively. The dissociation enthalpies were combined with the known heats of formation and electron affinities of the corresponding halocarbenes and other thermochemical data to give: $\Delta H_{f,298}(CH) = 142.2 \pm 3.2$, $\Delta H_{f,298}(CF) = 60.6 \pm 3.4$, and $\Delta H_{f,298}(CCl) = 105.9 \pm 3.1$ kcal/mol. The experimental results for all three carbynes are in good agreement with the predicted heats of formation obtained from G2 calculations. The measured values for CH and CF are in excellent agreement with other experimental values, whereas results for CCl do not support the heats of formation for this carbyne given in current thermochemical data compilations. The halogen substituent effects on carbyne stabilities and on the sequential C–H bond energies of CH_3F and CH_3Cl are shown to be dominated by π-donor interactions. (Int J Mass Spectrom 185/186/187 (1999) 745–757) © 1999 Elsevier Science B.V.

Keywords: Carbyne; Carbene anion; Thermochemistry; Collision-induced dissociation; Flowing afterglow

1. Introduction

Valuable new lessons about the interplay of electronic structure and thermochemistry have emerged from experimental and theoretical studies of reactive organic intermediates such as radicals, carbenes, and biradicals. Measurements of the absolute heats of formation for these species have allowed comparisons to be made of the first and second C–H bond energies for various organic molecules [1–8]. When two sequential C–H bond dissociations in a molecule produces a carbene or biradical fragment that has a singlet ground state, the second C–H bond is weaker than the first by an amount of energy that is directly related to the singlet–triplet splitting for the carbene or biradical [9,10]. When a triplet state carbene or biradical is formed, the second C–H bond dissociation energy is usually the same as or greater than the first. Delineating the trends in the magnitudes of the *third* C–H bond strengths of organic molecules requires accurate heats of formation for carbynes and triradicals—highly reactive species for which little or no

* Corresponding author (deceased 9/30/98).

Dedicated to Professor Michael T. Bowers on the occasion of his 60th birthday.

PII S1387-3806(99)14182-9

thermodynamic data are currently available. In this paper we present an application of the energy-resolved collision-induced dissociation method to the determination of absolute heats of formation for three simple carbynes, CH, CF, and CCl.

The archetypal carbyne, methylidyne (CH), is believed to play an important role in the formation of hydrocarbons in planetary atmospheres and interstellar clouds [11,12], and its reaction with molecular nitrogen is proposed as the initial step in "prompt NO" formation during hydrocarbon combustion [13]. The properties, reactivity, and spectroscopy of methylidyne are relatively well established. CH has a $^2\Pi$ ground state and a quartet excited state of $^4\Sigma^-$ symmetry lying 17.1 kcal/mol higher in energy [14]. CH is frequently compared to methylene (CH_2), which also has two low-lying electronic states: a triplet ground state of $^3B_1$ symmetry and a $^1A_1$ singlet excited state lying 9.0 kcal/mol higher in energy [15]. Doublet CH and singlet CH_2 share high reactivities, with measured rate coefficients for gas-phase reactions with small molecules that are essentially equal to the gas-kinetic limits [16,17]. Both molecules readily insert into the C–H bonds of saturated hydrocarbons, and they both undergo rapid cycloaddition to olefins [16,17]. The gas-phase reactivity of $^4\Sigma^-$ CH resembles that of $^3B_1$ CH_2 in that it reacts faster with open-shell molecules than with closed-shell molecules [18]. Methylidyne has an accurately known 298 K heat of formation of 142.6 ± 0.4 kcal/mol [19] that was derived from the spectroscopically determined value for D_0(CH) [20].

Halocarbynes such as fluoromethylidyne (CF) and chloromethylidyne (CCl) are present in plasmas used for silicon etching in the microelectronics industry [12,21]. Like methylidyne, CF and CCl also possess doublet ($^2\Pi$) ground states [22]. However, they are considerably less reactive than CH [23,24], because, as with singlet halocarbenes, π-donation by the halogen lone pairs greatly reduces the electrophilicity of the carbon p-orbitals, whereas electron withdrawal by the halogen stabilizes the nonbonding σ electron pair. For these same reasons, halocarbynes are predicted to have much larger doublet–quartet splittings than CH. Estimates for the doublet–quartet splittings for CF and CCl based on ab initio calculations range from 60–86 kcal/mol [25]. The 298 K heat of formation for CF is reasonably well-established at 61 ± 2 kcal/mol [26–28], but there is a discrepancy in the reported values for $\Delta H_{f,298}$(CCl). The earlier NIST thermochemical compilations [26] list a value of 92 kcal/mol, whereas a heat of formation of 120 ± 5 kcal/mol is given in the JANAF Tables [27]. The latest NIST compilation [28] recommends the JANAF value for $\Delta H_{f,298}$(CCl).

We have demonstrated [3,5,6] that accurate heats of formation for carbenes can be obtained from the measured threshold energies for collision-induced halide dissociation from α-halocarbanions [Eq. (1)]. In the present study, we extend this approach to the carbynes CH, CF, and CCl, by measuring the chloride dissociation energies for the corresponding halocarbene anions, $CHCl^{\cdot -}$, $CFCl^{\cdot -}$, and $CCl_2^{\cdot -}$ [Eq. (2)].

$$R_2CX^- \rightarrow R_2C + X^- \qquad X = Cl, Br, I \qquad (1)$$

$$CXCl^{\cdot -} \rightarrow CX + Cl^- \qquad X = H, F, Cl \qquad (2)$$

The thermochemical properties of these carbynes are also examined with ab initio calculations carried out at the G2 level of theory. The relative stabilities of CH, CF, and CCl are discussed, along with the substituent effects on the sequential C–H bond energies of CH_3X, X = H, F, Cl.

2. Experimental details

All experiments were carried out at room temperature (298 ± 2 K) in a flowing afterglow triple–quadrupole instrument that has been described in detail previously [29]. The pressure and flow rate of the helium buffer gas in the 1 m × 7.3 cm (id) flow tube were 0.4 Torr and 190 STP cm^3/s, respectively. Atomic oxygen anion, $O^{\cdot -}$, was formed in the upstream ion source region by dissociative ionization of N_2O. Halocarbene anions ($CXCl^{\cdot -}$, X = H, F, Cl) were generated by the reaction of $O^{\cdot -}$ with one of the halogen-substituted methanes, CH_3Cl, CH_2ClF, or CH_2Cl_2 [30], that was added to the flow reactor through a gas inlet located approximately 30 cm from

the ion source. Ions in the flow tube are thermalized by $\approx 10^5$ collisions with the helium buffer gas prior to tandem mass spectrometric analysis. For collision-induced dissociation (CID) experiments, negative ions are gently extracted from the flow tube through a 1 mm orifice into a region of differential pumping and then focused into the Extrel triple quadrupole mass analyzer. The desired reactant ion is mass selected with the first quadrupole, and then injected into the rf-only, gas-tight quadrupole collision chamber (Q2) with an axial kinetic energy controlled by the Q2 rod offset voltage. CID of the reactant ions is carried out in Q2 with either neon or argon target gas maintained at constant pressures corresponding to single-collision conditions (0.02–0.06 mTorr) [29]. Reactant and product ions are extracted from Q2 by a low-voltage exit lens into the third quadrupole that is held at a constant attractive voltage relative to the Q2 offset voltage. A conversion dynode and electron multiplier operating in pulse-counting mode are used for ion detection.

The data collection and analysis procedures used for CID threshold measurements have been described in detail [7,31]. In these experiments, the yield of a particular CID product ion is monitored while the axial kinetic energy of the reactant ion is scanned. A product ion appearance curve is generated by plotting the CID cross section versus the reactant ion-target collision energy in the center-of-mass (CM) frame, $E_{CM} = E_{LAB}[m/(M + m)]$, where E_{LAB} is the lab-frame energy, m is the mass of the neutral target, and M is the mass of the reactant ion. The energy axis origin is verified by retarding potential analysis, and the reactant ion kinetic energy distribution is generally found to have a near-Gaussian shape with a full-width at half-maximum of 0.5–1.5 eV. An uncertainty in the lab-frame energy scale of ± 0.1 eV ($\pm 1\sigma$ from replicate beam-zero measurements) is included in the total uncertainty of the reported thresholds. Absolute cross sections for the formation of a single product from CID, σ, are calculated by using the thin-target expression, $\sigma = I_p/INl$, where I_p and I are the measured intensities of the product and reactant ion signals, N is the number density of the target gas, and l is the effective collision path length for reaction (24 ± 4 cm) [29]. Phase incoherence between the quadrupolar fields in the triple quadrupole analyzer leads to oscillations in the apparent intensity of the reactant ion signal, but not the product ion signals, as the Q2 pole offset voltage is scanned. Accordingly, the intensity of the reactant ion beam is estimated to be equal to the maximum transmitted intensity in the region of the dissociation onset. This factor, as well as possible differences in the collection or detection efficiencies for the reactant and product ions, lead to inaccuracies in the absolute cross sections that have an estimated uncertainty of a factor of two. The relative cross sections have estimated uncertainties ±20%.

The threshold energy for dissociation is determined by fitting the product ion appearance curve with the model function given by Eq. (3) that takes into account the contribution to the total available energy from the reactant ion vibrational energy [32].

$$\sigma = \sigma_0 \sum_{i=1}^{3n-6} g_i(E + E_i - E_0)^n/E \quad (3)$$

In this expression, E_0 is the desired threshold energy, E is the center-of-mass collision energy, σ_0 is a scaling factor, n is an adjustable parameter, and i denotes reactant ion vibrational states having energy E_i and population g_i ($\Sigma g_i = 1$). The reactant ion vibrational energy distributions were estimated from scaled harmonic vibrational frequencies obtained from B3LYP/6-31G(d) calculations (scale factor = 0.972 [33]). The appearance curves are fit by an iterative procedure in which E_0, σ_0, and n are varied so as to minimize deviations between the data and the calculated cross sections in the steeply rising portion of the threshold region.* The experimental cross sections very near the actual reaction onset are not included in the fit because of the known deleterious effects of translational excitation and collisions of the reactant ions outside Q2 that can lead to pronounced "tails" in the appearance curves. Because the threshold is being derived from the experimental cross

* Analysis carried out by using the CRUNCH program written by Professor P.B. Armentrout and Professor K.M. Ervin.

sections measured at energies above the actual dissociation onset, we do not include a term in Eq. (3) for the rotational energy of the reactant ions [32], because, at these higher energies, the rotational energy is likely to be conserved on average during the collision with the target gas. A Doppler broadening function [34], which accounts for the random thermal motion of the target, and the kinetic energy distribution of the reactant ion approximated by a Gaussian function with a full-width at half-maximum of 1.5 eV (lab frame) are also convoluted together with the calculated cross sections obtained with Eq. (3). The threshold energies obtained in this manner correspond to 0 K bond dissociation energies. The 298 K dissociation enthalpies are derived by combining the 0 K bond energy with the calculated difference in 0–298 K integrated heat capacities of the dissociation products and reactants, plus a PV work term ($RT = 0.6$ kcal/mol at 298 K). The stationary electron convention is employed in this work [26].

The small size and relatively low dissociation energies of the halocarbene anions examined in this study suggest that dissociation of collisionally activated ions with sufficient internal energy should occur rapidly on the instrumental time scale ($\approx$30 μs) and, hence, kinetic shifts are unlikely. Fits of selected data sets with a modified form of Eq. (3) that explicitly accounts for possible kinetic shifts [35] show these effects to be entirely negligible for the halocarbene anions. This is consistent with previous energy-resolved CID studies involving relatively small halocarbanions with low halide dissociation energies [5].

Gas purities were as follows: He (99.995%), Ar (99.955%), N_2O (99.99%), Ne (99%), CH_3Cl (99.5%), CH_2ClF (99%). All liquid reagents were obtained from commercial sources and used as supplied except for degassing prior to use.

3. Computational details

Ab initio calculations were performed with the G2 method, which gives extrapolated total energies at the (U)QCISD(T)/6-311+G(3df,2p) level of theory for (U)MP2(full)/6-31G(d) optimized geometries [36]. Zero-point energies and 298 K enthalpy corrections were derived from scaled harmonic vibrational frequencies obtained at the (U)HF/6-31G(d) level (scale factor = 0.8929) [37]. Absolute heats of formation for CF and CCl were calculated by using the G2 atomization approach and the experimental heats of formation for C(g) and X(g) [38]. The 298 K heats of formation for CF and CCl were also estimated by combining the calculated enthalpy changes for the isodesmic and isogyric reaction shown in Eq. (4) with the experimental heats of formation for CH, CH_4, and CH_3X.

$$CX + CH_4 \rightarrow CH + CH_3X \qquad X = F, Cl \qquad (4)$$

The enthalpy change for Eq. (4) is referred to as the "carbyne stabilization energy," CySE, and it will also be used to quantify the halogen substituent effects in CF and CCl. In addition, chloride dissociation enthalpies for the three halocarbene anions, DH_{298}[CX–Cl$^-$], were calculated directly from the differences in G2 enthalpies for each species in Eq. (2). All of the G2 and DFT calculations were performed with use of the GAUSSIAN94 suite of programs [39] on an IBM RISC 6000.

4. Results

The present determination of the absolute heats of formation for CH, CF, and CCl is based on measurements of the chloride dissociation energies for $CHCl^{\cdot -}$, $CClF^{\cdot -}$, and $CCl_2^{\cdot -}$, respectively, by energy-resolved CID. The measured dissociation energies can be combined according to Eq. (5) with the known heats of formation and electron affinities of the corresponding halocarbenes, and with the well-established heat of formation for chloride ion in order to derive the heats of formation for the three carbynes.

$$\Delta H_{f,298}(CX) = DH_{298}[CX - Cl^-] + \Delta H_{f,298}(CXCl) - EA(CXCl) - \Delta H_{f,298}(Cl^-) \qquad (5)$$

The supplemental thermochemical data used for deriving the carbyne heats of formation and other properties reported in this work are given in Table 1.

Table 1
Supplemental thermochemical data

Compound	$\Delta H_{f,298}$ kcal/mol	Reference
C	171.3	[26]
H	52.1	[26]
F	19.0	[26]
Cl	29.0	[26]
CH	142.6 ± 0.4	[19]
CH_4	−17.83 ± 0.07	[59]
CH_3F	−56.8 ± 2.0	[49]
CH_3Cl	−19.6 ± 0.2	[26]
Cl^-	−54.4	[26]
$^1A_1$ CH_2	101.1 ± 0.5	[60]
$^3B_1$ CH_2	92.9 ± 0.6	[60]
CHCl	78.0 ± 2.0	[5]
CClF	7.4 ± 3.2	[5]
CCl_2	55.0 ± 2.0	[5]
	EA	eV
CHCl	1.210 ± 0.005	[45]
CClF	[1.001 ± 0.022]	[a]
CCl_2	1.603 ± 0.008	[46]
	DH_{298}[R–H]	
CH_4	104.9 ± 0.1	[1]
CH_3F	101 ± 1	[b]
CH_3Cl	100 ± 2	[c]

[a] Derived from G2 calculation (see text).
[b] Average of values from Holmes and Lossing [61] and McMillen and Golden [1].
[c] Average of values obtained from G2(MP2) calculations [5] and McMillen and Golden [1].

The halocarbene radical anions $CHCl^{\cdot -}$, $CClF^{\cdot -}$, and $CCl_2^{\cdot -}$ were generated in the flowing afterglow by $H_2^{\cdot -}$ abstraction from CH_3Cl, CH_2ClF, and CH_2Cl_2, respectively, by $O^{\cdot -}$. Carbene anion formation is the major primary reaction for all three halomethanes [30,40]. Lesser amounts of Cl^- and OH^- are produced as primary reaction products, and the halomethyl anions $CHClF^-$ and $CHCl_2^-$ are also formed in the case of CH_2ClF and CH_2Cl_2, respectively. Collision-induced dissociation of $CHCl^{\cdot -}$, $CClF^{\cdot -}$, and $CCl_2^{\cdot -}$ with either argon or neon target gas produces Cl^- as the only ionic fragment in the 1–30 eV (lab) collision energy range [Eq. (2)]. The maximum CID cross sections for the three ions are in the range of 2–4 Å^2 at ≈5 eV (CM), with apparent dissociation onsets less than 2 eV.

Initial CID measurements with $CHCl^{\cdot -}$ by using either argon or neon target gas revealed nonzero cross sections at low kinetic energies, as shown in Fig. 1(a) for argon target. This low-energy feature is characteristic of an exothermic reaction by $CHCl^{\cdot -}$ that produces Cl^-. Replacing the rare gas target with pure oxygen results in a Cl^- appearance curve with a maximum cross section of ∼5 Å^2 at kinetic energies less than 0.5 eV, as shown in Fig. 1(b). Likewise, deliberate addition of small amounts of O_2 to the argon target gas in Q2 enhances the low-energy feature that is present in Fig. 1(a). This indicates that Cl^- is produced by an exothermic ion/molecule reaction between $CHCl^{\cdot -}$ and O_2 [Eq. (6)].

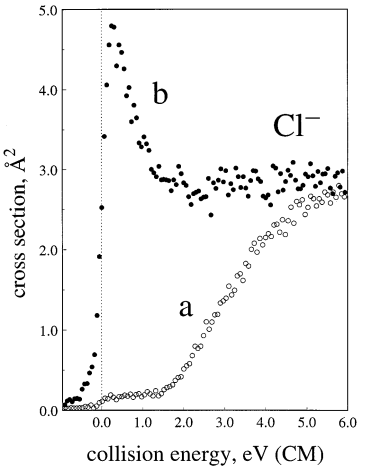

Fig. 1. Chloride ion appearance curve resulting from (a) collision-induced dissociation of $CHCl^{\cdot -}$ with argon target containing a trace amount of O_2 impurity (P_{total} = 4 × 10^{-5} Torr), and (b) reaction/CID of $CHCl^{\cdot -}$ with pure oxygen target at 4 × 10^{-5} Torr.

$$CHCl^{\cdot -} + O_2 \rightarrow Cl^- + [C,H,2O] \quad (6)$$

We therefore attribute the nonzero cross section below the CID onset in Fig. 1(a) to unavoidable traces of O_2 contamination in the target gas that results in an exothermic reaction yielding Cl^-. Thermochemical estimates indicate that the neutral product or products of Eq. (6) could be any [C,H,2O] isomer or collection of [C,H,2O] products with a total enthalpy less than ≈105 kcal/mol, including formoxyl radical, dioxiranyl radical, CO_2 + H, CO + OH, or even CO + O + H [28]. Similar behavior was observed in our recent energy-resolved CID measurements with CH_2Cl^- and CH_2Br^-—minute traces of O_2 impurities

in the argon and neon target gas also produced low-energy features in the halide ion appearance curves due to exothermic ion/molecule reactions [6].

The low-energy feature is of sufficient intensity throughout the region of the CID onset for $CHCl^{\cdot -}$ to obscure the threshold analysis. This feature can, in principle, be eliminated by linearly extrapolating to zero O_2 impurity the cross sections obtained with deliberate addition of varying amounts of oxygen to the argon target gas. However, the exothermic reaction between $CHCl^{\cdot -}$ and O_2 is evidently so efficient relative to CID that the very small amounts of oxygen "spiking" required for a reliable extrapolation to zero impurity are difficult achieve with our target gas inlet system.

A better approach is to eliminate the low-energy feature by deconvolution. For these experiments, Cl^- appearance curves were obtained by using pure oxygen as the target gas, such as the one shown in Fig. 1(b). The pure-O_2 cross sections were then scaled to the maximum cross section in the low energy region of the Cl^- appearance curves obtained with (impure) argon as the collision gas. Subtracting of the scaled-O_2 cross sections from the impure-argon cross sections gives a Cl^- appearance curve corresponding to pure argon target in which the exothermic O_2 reaction feature has been eliminated. An example of a deconvoluted appearance curve obtained in this way is shown in Fig. 2. This procedure is similar to the one used by Armentrout and co-workers to analyze the CID thresholds for $M(C_6H_6)_2^+$ ions [41]. In this case, low-energy features in the $M(C_6H_6)^+$ appearance curves arose from electronically excited species in the reactant ion beam that had lower dissociation energies than the ground-state metal ions. These low-energy features were fit with a model similar to Eq. (3), and the resulting model cross sections were subtracted from the experimental appearance curves prior to analysis of the higher energy thresholds. For $Cr(C_6H_6)_2^+$, it was found that the CID thresholds obtained by deconvoluting the low-energy features compared favorably with those derived from appearance curves obtained with use of alternative ion sources that did not produce excited-state impurities.

A series of Cl^- appearance curves from CID of

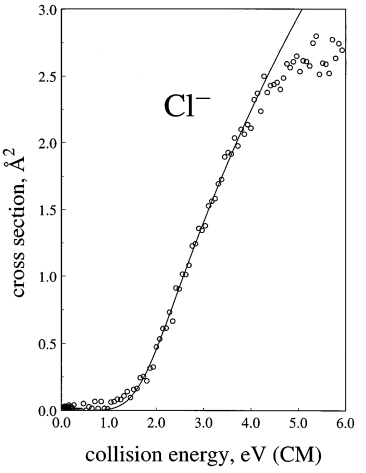

Fig. 2. Deconvoluted Cl^- appearance curve obtained by subtracting the scaled cross sections in Fig. 1(b) from the cross sections in Fig. 1(a). The solid line is the optimized, fully convoluted model appearance curve obtained with Eq. (3).

$CHCl^{\cdot -}$ with argon target were collected and deconvoluted as described above. The data were modeled with Eq. (3) in the prescribed manner, and average values were obtained for the threshold energy E_0 and the fitting parameter n of 1.60 ± 0.10 eV and 1.46 ± 0.07, respectively. The uncertainty in E_0 represents the root-square sum of the standard deviation ($\pm 1\sigma$) of 13 replicate measurements, and the ±0.1 eV (lab) uncertainty in the energy scale. The parameter n is related to the shape of the CID cross section, and it has generally ranged from 1.3 to 1.8 for other halocarbanion dissociations examined in our laboratory [5–7]. Analogous measurements and deconvolution analyses were carried out for CID of $CHCl^{\cdot -}$ with neon target gas. The average threshold value obtained from 32 different data sets is 1.59 ± 0.11 eV (n = 1.41 ± 0.12), in excellent agreement with the results obtained with argon target gas. The pooled average of all the data is 1.59 ± 0.11 eV (n = 1.42 ± 0.11). Possible systematic errors that may arise from inadequacy of the threshold function and uncertainty in the reactant ion vibrational frequencies are negligibly small compared to the random errors, and are not included in the final uncertainty.

Representative cross sections for energy-resolved CID of $CClF^{\cdot -}$ with neon target gas and for $CCl_2^{\cdot -}$

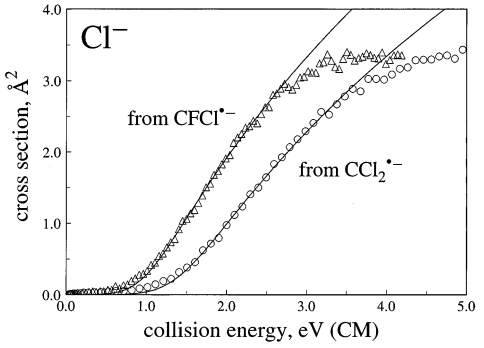

Fig. 3. Cross section for the dissociation of chloride from $CFCl^{\cdot -}$ (open triangle) and $CCl_2^{\cdot -}$ (open circle) resulting from collisional activation with neon and argon targets, respectively ($P = 4 \times 10^{-5}$ Torr). The solid lines are the optimized, fully convoluted model appearance curve obtained with Eq. (3).

with argon target gas are shown in Fig. 3. Unlike $CHCl^{\cdot -}$, the dihalocarbene ions do not exhibit low-energy, high-yield features in their Cl^- appearance curves, which indicates that reactions of these ions with the trace O_2 impurity in the target gas are less favorable.* Neon target gas was used for the CID measurements with $CFCl^{\cdot -}$ because of its relatively low CID onset. Neon is the preferred CID target for ions with dissociation energies less than about 1 eV, because higher laboratory collision energies may be used for a given center-of-mass collision energy compared to argon or xenon. This has the advantage of increasing the separation between the reactant ion transmission cutoff and CID onset regions in the laboratory frame energy scale [42]. Analysis of 17 different Cl^- appearance curves obtained from CID of $CFCl^{\cdot -}$ with neon target gives average values for E_0 and n of 0.92 ± 0.05 eV and 1.52 ± 0.06, respectively, where the uncertainty in E_0 is derived in the previously described manner.

Analysis of the Cl^- appearance curves obtained from CID of $CCl_2^{\cdot -}$ with argon and with neon reveals a significant target gas effect. The average values for E_0 and n obtained from 12 CID threshold measurements with neon target are 1.68 ± 0.04 eV and 1.55 ± 0.04, respectively, whereas 38 different measurements with argon target give average values of 1.43 ± 0.10 eV and 1.46 ± 0.05, respectively. A few measurements with use of xenon target were carried out that give an average threshold of 1.4 eV.† The 0.25 eV difference between the values of E_0 obtained with neon and argon targets is statistically significant, and in a direction that suggests inefficient collisional energy transfer with the lighter neon target [43,44]. That is, the internal energy imparted to $CCl_2^{\cdot -}$ upon collision with neon at the nominal dissociation threshold is too low, so a shift in the reaction onset to higher energy results. With the heavier, more polarizable argon target, the collision energy is more effectively transformed into internal energy of the $CCl_2^{\cdot -}$ ions, such that the dissociation rate is much larger at the thermochemical threshold. It is remarkable that $CCl_2^{\cdot -}$ exhibits a target effect, whereas $CHCl^{\cdot -}$ does not, despite the slightly higher dissociation energy of the latter. The 71% greater mass of $CCl_2^{\cdot -}$ relative to $CHCl^{\cdot -}$ is evidently the key factor. The lower threshold for CID of $CCl_2^{\cdot -}$ obtained with argon target gas is taken to be the correct one.

Combining the measured values of E_0 for the three ions with the calculated differences in 0–298 K integrated heat capacities for the dissociation products and reactants gives chloride dissociation enthalpies, $DH_{298}[CX–Cl^-]$, of 37.7 ± 2.3, 21.9 ± 1.1, 33.4 ± 2.3 kcal/mol for X = H, F, and Cl, respectively. A summary of the energy-resolved CID results is given in Table 2.

In order to derive carbyne heats of formation from the chloride dissociation enthalpies of the halocarbene anions, heats of formation and electron affinities (EA) for the corresponding neutral halocarbenes are required [Eq. (5)]. The recommended values for the 298 K heats of formation of CHCl, CClF, and CCl_2 are

* The reactions of $CFCl^{\cdot -}$ and $CCl_2^{\cdot -}$ with pure O_2 target gas produce Cl^- with maximal cross sections at collision energies around 0.4 eV (CM) that are less than 19% and 13%, respectively, of the maximum CID cross sections at 4 eV. Product ions formed at low collision energies from the reaction between O_2 and $CCl_2^{\cdot -}$ are Cl^-, $Cl_2^{\cdot -}$, and $Cl_2O^{\cdot -}$, whereas $CFCl^{\cdot -}$ produces only Cl^-.

† Although the CID thresholds obtained with use of argon target for $CFCl^{\cdot -}$ and xenon target for $CCl_2^{\cdot -}$ are consistent with the neon and argon results, respectively, the Cl^- appearance curves measured with the heavier targets display greater tailing in the threshold regions, which leads to less reliable modeling and reduced precision.

Table 2
Experimental thermochemical data for carbynes

CX	$E_0(CXCl^-)$[a] eV	n[b]	$DH_{298}[CX–Cl^-]$ kcal/mol	$\Delta H_{f,298}(CX)$[c] kcal/mol
CH	1.60 ± 0.10	1.46 ± 0.07	37.7 ± 2.3	142.2 ± 3.2
CF	0.92 ± 0.05	1.52 ± 0.06	21.9 ± 1.1	60.6 ± 3.4
CCl	1.43 ± 0.10	1.46 ± 0.05	33.4 ± 2.3	105.9 ± 3.1

[a] CID threshold energy, Eq. (2).
[b] Optimized shape parameter, Eq. (3).
[c] Eq. (5).

78.0 ± 2.0, 7.4 ± 3.2, and 55.0 ± 2.0 kcal/mol, respectively [5]. The electron affinities of CHCl and CCl_2 have been determined by negative ion photoelectron spectroscopy to be 1.210 ± 0.005 eV and 1.603 ± 0.008 eV, respectively [45,46]. The electron affinity of CClF has not been determined experimentally, but it can be reliably estimated from G2 calculations. Electron affinities were computed for all of the chlorosubstituted and fluorosubstituted carbenes from the differences in the (0 K) G2 energies of the corresponding negative ions and neutral molecules. Table 3 compares the calculated electron affinities with the experimental values. G2 theory systematically underestimates the electron affinities by an average of 0.103 eV. This correction factor was applied to the calculated EA value for CClF (0.898 eV) to give a final estimate of 1.001 ± 0.022 eV, where the assigned uncertainty is the standard deviation of the average correction factor. Combining the measured chloride dissociation enthalpies with the carbene heats of formation and electron affinities, and $\Delta H_{f,298}(Cl^-)$ according to Eq. (5) gives 298 K heats of formation for CH, CF, and CCl of 142.2 ± 3.2, 60.6 ± 3.4, and 105.9 ± 3.1 (Table 2). The assigned uncertainties are computed from the root-square sum of the uncertainties in each term of Eq. (5).

4.1. Theoretical results

Theoretical estimates of the carbyne heats of formation and halocarbene anion dissociation energies were obtained from G2 calculations. The calculated 298 K heats of atomization for the doublet ground states of CH, CF, and CCl were computed, and then combined with the experimental heats of formation of the corresponding gaseous atoms to give the $\Delta H_{f,298}(CX)$ values listed in Table 4. For CF and CCl, 298 K heats of formation were also derived from the computed enthalpy changes for the isodesmic reaction indicated by Eq. (4), and the known heats of formation for CH, CH_4, CH_3F, and CH_3Cl. The agreement between the results obtained with the two approaches is good, although the heats of formation derived from atomization enthalpies are slightly lower

Table 3
Calculated and experimental electron affinities of halocarbenes[a]

Carbene	EA(G2)[b]	EA(exp)	EA(exp)–EA(G2)	Reference
CHCl	1.102	1.210 ± 0.005	0.108	[45]
CHF	0.462	0.542 ± 0.005	0.080	[45]
CCl_2	1.467	1.603 ± 0.008	0.136	[46]
CF_2	0.092	0.179 ± 0.005	0.087	[46]
CClF	0.898	[1.001 ± 0.022][c]	[0.103][d]	this work

[a] All values in eV.
[b] Computed directly from differences in 0 K G2 energies of anion and neutral.
[c] Corrected G2 electron affinity for CClF. The indicated uncertainty is the standard deviation of the average correction factor.
[d] Average difference between calculated and experimental electron affinities for CHCl, CHF, CCl_2, and CF_2.

Table 4
Thermochemical quantities derived from G2 calculations[a]

CX	$\Delta H_{f,298}$ (atomization)[b]	$\Delta H_{f,298}$ (isodesmic)[c]	$\Delta H_{f,298}$ (average)[d]	DH_{298} [CX–Cl$^-$][e]
CH	142.0	—	142.0 (0.6)	37.7 (0.0)
CF	57.7	59.0	58.4 (2.2)	18.8 (3.1)
CCl	103.6	104.2	103.9 (2.0)	29.4 (4.0)

[a] All values in kcal/mol; deviation from experimental values shown in parentheses.
[b] Heat of formation derived from enthalpy of atomization.
[c] Heat of formation derived from enthalpy of isodesmic reaction, Eq. (4).
[d] Average heat of formation obtained from atomization and isodesmic reaction approaches.
[e] Calculated from the differences in G2 enthalpies of products and reactants, Eq. (2).

than those derived with use of Eq. (4). A similar systematic deviation was evident in the G2-derived heats of formation for halocarbenes obtained from atomization versus isodesmic reaction enthalpies [5]. The Cl^- dissociation enthalpies for $CHCl^{\cdot -}$, $CFCl^{\cdot -}$, and $CCl_2^{\cdot -}$ were also computed from the G2 enthalpies of the products and reactants of Eq. (2). These are listed in the last column of Table 4.

5. Discussion

The halide dissociation reactions that produce carbynes from α-halocarbene anions [Eq. (2)] and halocarbenes from α-halocarbanions [Eq. (1)] are analogous in several respects. Both reactions are spin- and symmetry-allowed, occurring on single diabatic potential energy surfaces. Hence, there are no curve crossings that may produce electronic barriers in excess of the reaction endothermicity. The reverse reactions, nucleophilic additions to singlet carbenes [47] and doublet carbynes [48], have been shown to occur without barriers. Therefore, the activation energies for dissociation determined by the CID threshold experiments can be equated with the thermochemical bond energies.

Like the halomethyl carbanions examined in our recent carbene study [5], the halomethylene anions examined in the present work all have electron binding energies that are similar in magnitude to their chloride dissociation energies (cf. Tables 2 and 3). This makes competitive shifts in the CID onsets due to collision-induced electron detachment unlikely, because these effects appear to be important only when the dissociation energy exceeds the electron binding energy of the reactant anion by a large margin ($\geq$1 eV) [3,6,7,31]. The maximum CID cross sections measured for the three halomethylene anions are in the same range, 2–4 Å^2, as those determined for halomethyl carbanions [5]. If collision-induced electron detachment of the reactant ions represented a significant decomposition channel, then much lower CID cross sections would result [3].

The 298 K heat of formation for CH determined in this work, 142.2 $\pm$ 3.2 kcal/mol, is in excellent agreement with the value of 142.6 $\pm$ 0.4 kcal/mol derived by Ervin et al. [19] from the spectroscopically determined value for D_0(CH) = 79.9 $\pm$ 0.4 kcal/mol reported by Helm et al. and by Brzozowski et al. [20]. G2 calculations give a 298 K atomization energy for CH of 81.4 kcal/mol that leads to $\Delta H_{f,298}$(CH) = 142.0 kcal/mol. There is also good agreement between the heat of formation for CF determined in this work by CID, 60.6 $\pm$ 3.4 kcal/mol, and the value recommended in the JANAF compilation, 61 $\pm$ 2 kcal/mol [27], that is based on a critical evaluation of results from several different high-temperature equilibrium and spectroscopic measurements. The predicted value for $\Delta H_{f,298}$(CF) obtained from G2 calculations is 58.4 kcal/mol (Table 4), which is about 2.5 kcal/mol lower than the experimental values. Berry and co-workers have noted that the absolute heats of formation predicted by G2 theory for chlorofluoromethanes are systematically low compared to experimental values by 2–3 kcal/mol [49]. The heats of formation for chlorosubstituted and fluorosubstituted carbenes derived from G2 theory also appear to be systematically low by similar amounts [5]. The 2.5 kcal/mol difference between the experimental and G2 estimates for $\Delta H_{f,298}$(CF) suggests a similar deficiency of G2 theory in predicting halocarbyne thermochemistry.

The value for $\Delta H_{f,298}$(CCl) obtained in this study, 105.9 $\pm$ 3.1 kcal/mol, is halfway between the value recommended in the JANAF tables, 120 $\pm$ 5 kcal/

mol [27], and the value listed in the earlier NIST compilations, 92 kcal/mol [26]. The JANAF value was derived from the flame spectroscopy results of Miller and Palmer [50], whereas the NIST value was derived by subtracting the measured ionization energy of CCl [51] from a value for the heat of formation for CCl^+ of unspecified origins. A heat of formation for CCl of 104 kcal/mol was estimated by Lias et al. by assuming that the bond energy of CCl was the same as the average C–Cl bond energy of CCl_2 [52]. However, this estimate made use of an incorrect heat of formation for CCl_2 that was too low by 16 kcal/mol [5]. Recalculating the estimate of Lias et al. with the correct heat of formation for CCl_2 [5] gives $\Delta H_{f,298}(CCl) = 113$ kcal/mol. The G2 prediction for $\Delta H_{f,298}(CCl)$ is 103.9 kcal/mol, and MP4SDTQ and QCISD calculations reported by Hopkinson and coworkers give similar values of 105.1 and 104.3 kcal/mol, respectively [53,54]. The theoretical estimates provide good support for the experimental value for $\Delta H_{f,298}(CCl)$ obtained in this study, and all of these results suggest that the JANAF- and NIST-recommended values are too high and too low, respectively. In considering possible sources of error in the previous literature values, we note that several questionable assumptions were made in deriving the high value for $\Delta H_{f,298}(CCl)$ given in the JANAF tables. The low value for $\Delta H_f(CCl)$ listed in the NIST compilation probably results from error in the heat of formation of CCl^+ that was used.

The chloride dissociation enthalpies for $CFCl^{\cdot -}$ and $CCl_2^{\cdot -}$ predicted by G2 theory are lower than the experimental values by 3.1 and 4.0 kcal/mol, respectively, whereas experiment and theory are in excellent agreement for $DH_{298}[CH–Cl^-]$ (Table 4). Similar discrepancies were noted between the measured and calculated chloride dissociation enthalpies of halomethyl carbanions [5]. These discrepancies are merely another manifestation of the erroneously low heats of formation predicted by G2 for halocarbenes and halocarbynes.

We can use the experimental data for CH, CF, and CCl to evaluate the halogen substituent effects on carbyne thermochemistry [55]. The carbyne stabilization energy (CySE) defined by Eq. (4) is analogous to the carbene stabilization energy (CSE) [56], which is defined as the enthalpy change for Eq. (7), and the radical stabilization energy (RSE) [57], as defined by the enthalpy change for Eq. (8).

Table 5
Substituent stabilization enthalpies[a]

Substituent	RSE[b]	Singlet-CSE[c]	Triplet-CSE[c]	CySE[d]
F	3.0	27.9	4.8	43.0
Cl	4.0	21.3	8.9	34.9

[a] All values in kcal/mol; derived from experimental data listed in Tables 1 and 2.
[b] Eq. (8).
[c] Eq. (7).
[d] Eq. (4).

$$(^1A' \text{ or } ^3A'')CHX + CH_4 \rightarrow (^1A_1 \text{ or } ^3B_1)CH_2 + CH_3X \qquad X = F, Cl \quad (7)$$

$$CH_2X + CH_4 \rightarrow CH_3 + CH_3X \qquad X = F, Cl \quad (8)$$

Different CSE values for singlet and triplet carbenes can be derived, because the absolute heats of formation and S–T splittings of CH_2, CHF, and CHCl are known [15,45]. Values of CySE, RSE, and singlet- and triplet-CSE are listed in Table 5. It is immediately evident that the substituent effects are largest for carbynes and smallest for radicals, and that there is a large difference between the substituent effects for singlet and triplet carbenes. Moreover, fluorine exhibits a larger stabilizing effect than chlorine in singlet carbenes and carbynes, but a smaller effect in radicals and triplet carbenes. These trends are easily understood in terms of π-donation effects. When the unsaturated carbon possesses an empty p-π orbital, as in doublet carbynes and singlet carbenes, the superior π-donor ability of fluorine compared to chlorine leads to greater relative stabilization in the fluorinated species. When the p-π orbital is singly occupied, as in the radicals and triplet carbenes, π-donation is less favorable so chlorine displays a larger stabilizing effect than fluorine. The larger halogen substituent effects for carbynes compared to singlet carbenes arise, in part, from better stabilization by the electrongative halogen of the sp-type lone pair in carbynes than the sp^2-type lone pair in singlet carbenes. Also, carbon–

Table 6
Sequential bond enthalpies for CH_4, CH_3F, and CH_3Cl[a]

DH_{298}	X = H	X = F	X = Cl
[CXH_2–H]	104.9 ± 0.1	101.0 ± 1.0	100.0 ± 2.0
[CXH–H]	110.0 ± 0.6	94.2 ± 3.7	101.8 ± 2.8
[CX–H]	101.8 ± 0.6	78.5 ± 4.5	80.0 ± 3.7
[C–X]	80.8 ± 0.6	129.7 ± 3.5	94.4 ± 3.2

[a] All values in kcal/mol; derived from experimental data listed in Tables 1 and 2.

halogen π-interactions are more stabilizing in carbynes compared to carbenes, because the carbon p-π orbitals in the former species are lower in energy than those in the latter (a carbyne carbon atom is more electronegative than a carbene carbon atom).

Complete listings of the sequential C–H (and C–X) bond strengths for CH_4, CH_3F, and CH_3Cl are given in Table 6. The origins of the trends in the first two C–H bond strengths for these compounds have been discussed previously [2,5,9]. The small decrease in the bond enthalpies for CH_3F and CH_3Cl compared to methane results from the weakly stabilizing three-electron π-interactions between the halogen lone pairs and the singly occupied carbon 2*p* orbital. The large reductions in the C–H bond strengths of CH_2F and CH_2Cl compared to CH_3 are caused by the energy released upon electronic relaxation of the halocarbenes to their singlet ground states. The third C–H bond energies of CH_3F and CH_3Cl are about the same (~79 kcal/mol), and are 16–22 kcal/mol lower than the second C–H bond energies. The bond strength reduction is due to the rehybridization of the lone-pair orbital from ~sp^2 to *sp* that accompanies dissociation [58], and the stronger π-interaction in the halocarbynes compared to halocarbenes. The third C–H bond energy of CH_4 is considerably greater (101.8 kcal/mol) than those of CH_3F and CH_3Cl. However, one should actually consider the bond energy for dissociation of *singlet* CH_2, 93.6 kcal/mol, which is lower by roughly the S–T splitting. The remaining 14–15 kcal/mol difference between the bond strengths in $^1CH_2$ versus ^1CHF and ^1CHCl is mainly attributable to π-stabilization effects in the halocarbynes.

6. Conclusions

Energy-resolved collision-induced dissociation of the halocarbene anions $CHCl^{\cdot -}$, $CClF^{\cdot -}$, and $CCl_2^{\cdot -}$ provides a means to determine accurate heats of formation for CH, CF, and CCl, respectively. The measured values for all three carbynes are in good agreement with predictions based on G2 calculations. The heats of formation obtained for CH and CF in this study are in excellent accord with established literature values, whereas the results for CCl suggest that the values for $\Delta H_{f,298}$(CCl) given in the JANAF and NIST thermochemical data compilations are incorrect. Analysis of the halogen substituent effects on carbyne stability and on the sequential C–H bond energies of CH_3F and CH_3Cl shows that π-interactions dominate these effects.

Future applications of this approach to other carbynes will depend upon the availability of absolute heats of formation and electron affinities for appropriate halocarbenes. Experimental efforts to expand this thermochemical database are currently in progress.

Acknowledgements

This work was supported by the National Science Foundation. We thank Jianhua Ren for her assistance with some of the CID threshold measurements.

References

[1] D.F. McMillen, D.M. Golden, Annu. Rev. Phys. Chem. 33 (1982) 493; J. Berkowitz, D. Gutman, G.B. Ellison, J. Phys. Chem. 98 (1994) 2744.
[2] P. Chen, Advances in Carbene Chemistry, Vol. 1, U.H. Brinker (Ed.), JAI, Greenwich, CT, 1994.
[3] J.A. Paulino, R.R. Squires, J. Am. Chem. Soc. 113 (1991) 5573.
[4] L.J. Chyall, R.R. Squires, Int. J. Mass Spectrom. Ion Processes 149/150 (1995) 257.
[5] J.C. Poutsma, J.A. Paulino, R.R. Squires, J. Phys. Chem. A 101 (1997) 5327.
[6] J.C. Poutsma, J.J. Nash, J.A. Paulino, R.R. Squires, J. Am. Chem. Soc. 119 (1997) 4686.
[7] P.G. Wenthold, R.R. Squires, J. Am. Chem. Soc. 116 (1994) 6401; 116 (1994) 7378.
[8] X. Zhang, P. Chen, J. Am. Chem. Soc. 114 (1992) 3147.

[9] E.A. Carter, W.A. Goddard III, J. Phys. Chem. 90 (1986) 998.
[10] J.A. Blush, H. Clauberg, D.W. Kohn, D.W. Minsek, X. Zhang, P. Chen, Acc. Chem. Res. 25 (1992) 385.
[11] A. Canosa, I.R. Sims, D. Travers, I.W.M. Smith, B.R. Rowe, Astron. Astrophys. 323 (1997) 644; Y. Sonoda, S. Iwata, Y. Osamura, Bull. Chem. Soc. Jpn. 66 (1993) 3345.
[12] M.A. Weibel, T.D. Hain, T.J. Curtiss, J. Chem. Phys. 108 (1998) 3134, and references therein.
[13] J.A. Miller, C.T. Bowman, Prog. Energy Combust. Sci. 15 (1989) 287, and references therein.
[14] A. Kasden, E. Herbst, W.C. Lineberger, Chem. Phys. Lett. 31 (1975) 78.
[15] A.R.W. McKeller, P.R. Bunker, T.J. Sears, K.M. Evenson, R.J. Saykally, S.R. Langhoff, J. Chem. Phys. 79 (1983) 5251; D.G. Leopold, K.K. Murray, A.E. Stevens-Miller, W.C. Lineberger, ibid. 83 (1985) 4849.
[16] M.R. Berman, J.W. Fleming, A.B. Harvey, M.C. Lin, Chem. Phys. 73 (1982) 27; K.H. Becker, B. Engelhardt, P. Wiesen, K.D. Bayes, Chem. Phys. Lett. 154 (1989) 342.; S. Zabarnick, J.W. Fleming, M.C. Lin, Int. J. Chem. Kinet. 21 (1989) 765.
[17] H. Frances, G.J. Gutsche, W.D. Lawrance, W.S. Staker, K.D. King, Combust. Flame 100 (1995) 653; A.O. Langford, H. Petek, C.B. Moore, J. Chem. Phys. 78 (1983) 6650.
[18] A.H. Laufer, Rev. Chem. Intermed. 4 (1981) 225; Z. Hou, K.D. Bayes, J. Phys. Chem. 96 (1992) 5685.
[19] K.M. Ervin, S. Gronert, S.E. Barlow, M.K. Giles, A.G. Harrison, V.M. Bierbaum, C.H. DePuy, W.C. Lineberger, G.B. Ellison, J. Am. Chem. Soc. 112 (1990) 5750.
[20] H. Helm, P.C. Cosby, M.M. Graff, J.T. Mosely, Phys. Rev. A 25 (1982) 304; J. Brzozowski, P. Bunker, N. Elander, P. Erman, Astrophys. J. 207 (1976) 414.
[21] J.P. Booth, G. Hancock, N.D. Perry, Appl. Phys. Lett. 50 (1987) 318; R.A. Gottscho, T.A. Miller, Pure Appl. Chem. 56 (1984) 189; S.G. Hansen, G. Luckman, S.D. Colson, Appl. Phys. Lett. 53 (1988) 1588.
[22] K.P. Huber, G. Herzberg, Molecular Spectra and Molecular Structure. IV. Constants of Diatomic Molecules, Van Nostrand Reinhold, New York, NY, 1979.
[23] J. Peeters, J. Van Hoeymissen, S. Vanhaelemeersch, D. Vermeylen, J. Phys. Chem. 96 (1992) 1257; J. Van Hoeymissen, I. De Boelpaep, W. Uten, J. Peeters, ibid. 98 (1994) 3725; I. De Boelpaep, B. Vetters, J. Peeters, J. Phys. Chem. A 101 (1997) 787.
[24] M. Rahman, M.L. McKee, P.B. Shevlin, J. Am. Chem. Soc. 108 (1986) 6296; C.J. LaFrancois, P.B. Shevlin, ibid. 116 (1994) 9405; R. Sztyrbicka, M.M. Rahman, M.E. D'Aunoy, P.B. Shevlin, ibid. 112 (1990) 6712; C.J. LaFrancois, P.B. Shevlin, Tetrahedron 53 (1997) 10071.
[25] G.L. Gustev, T. Ziegler, J. Phys. Chem. 95 (1991) 7220; T.H. Dunning, W.P. White, R.M. Pitzer, C.W. Mathews, J. Mol. Spectrosc. 75 (1979) 297; J.A. Hall, W.G. White, Mol. Phys. 23 (1972) 331.
[26] S.G. Lias, J.E. Bartmess, J.F. Liebman, J.L. Holmes, R.D. Levin, W.D. Mallard, J. Phys. Chem. Ref. Data 17 (1988), Suppl. 1. Updated in: J.E. Bartmess, NIST Standard Reference Database No. 19B (Negative Ion Energetics Database version 3.00), October 1993 Release, S.G. Lias, J.F. Liebman, R.D. Levin, S.A. Kafafi, NIST Standard Reference Database No. 25 (Positive Ion Energetics Database version 2.02), January 1994 release.
[27] M.W. Chase, C.A. Davies, J.R. Downey, D.J. Frurip, R.A. McDonald, A.N. Syverud, J. Phys. Chem. Ref. Data 14 (1985) Suppl. 1 (JANAF Tables).
[28] W.G. Mallard (Ed.), NIST Chemistry Webbook, NIST Standard Reference Database No. 69, March 1998 Release (http://nist.webbook.gov).
[29] P.J. Marinelli, J.A. Paulino, L.S. Sunderlin, P.G. Wenthold, J.C. Poutsma, R.R. Squires, Int. J. Mass Spectrom. Ion Processes 130 (1994) 89.
[30] J. Lee, J.J. Grabowski, Chem. Rev. 92 (1992) 1611, and references therein.
[31] L.S. Sunderlin, D. Wang, R.R. Squires, J. Am. Chem. Soc. 114 (1992) 2788; 115 (1993) 12060.
[32] W.J. Chesnavich, M.T. Bowers, J. Phys. Chem. 83 (1985) 900; L.S. Sunderlin, P.B. Armentrout, Int. J. Mass Spectrom. Ion Processes 94 (1989) 149; R.H. Schultz, K.C. Crellin, P.B. Armentrout, J. Am. Chem. Soc. 113 (1991) 8590.
[33] J.J. Nash, R.R. Squires, J. Am. Chem. Soc. 118 (1996) 8871.
[34] P.J. Chantry, J. Chem. Phys. 55 (1971) 2746.
[35] F.A. Khan, D.E. Clemmer, R.H. Schultz, P.B. Armentrout, J. Phys. Chem. 97 (1993) 7978.
[36] L.A. Curtiss, K. Raghavachari, G.W. Trucks, J.A. Pople, J. Chem. Phys. 94 (1991) 7221.
[37] J.A. Pople, A.P. Scott, M.W. Wong, L. Radom, Isr. J. Chem. 33 (1993) 345.
[38] A. Nicolaides, A. Rauk, M.N. Glukhovtsev, L. Radom, J. Phys. Chem. 100 (1996) 17460.
[39] GAUSSIAN94, version D.2, M.J. Frisch, G.W. Trucks, H.B. Schlegel, P.M.W. Gill, B.G. Johnson, M.A. Robb, J.R. Cheeseman, T. Keith, G.A. Petersson, J.A. Montgomery, K. Raghavachari, M.A. Al-Laham, V.G. Zakrzewski, J.V. Ortiz, J.B. Foresman, J. Cioslowski, B.B. Stefanov, A. Nanayakkara, M. Challacombe, C.Y. Peng, P.Y. Ayala, W. Chen, M.W. Wong, J.L. Andres, E.S. Replogle, R. Gomperts, R.L. Martin, D.J. Fox, J.S. Binkley, D.J. Defrees, J. Baker, J.P. Stewart, M. Head-Gordon, C. Gonzalez, J.A. Pople, Gaussian, Inc., Pittsburgh PA, 1995.
[40] M. Born, I. Ingemann, N.M.M. Nibbering, J. Am. Chem. Soc. 116 (1994) 7210.
[41] F. Meyer, F.A. Khan, P.B. Armentrout, J. Am. Chem. Soc. 117 (1995) 9740.
[42] L.S. Sunderlin, R.R. Squires, Chem. Phys. Lett. 212 (1993) 307.
[43] S.K. Loh, D.A. Hales, L. Lian, P.B. Armentrout, J. Chem. Phys. 90 (1989) 5466.
[44] D.A. Hales, P.B. Armentrout, J. Cluster Sci. 1 (1990) 127.
[45] M.K. Gilles, K.M. Ervin, J. Ho, W.C. Lineberger, J. Phys. Chem. 96 (1992) 1130.
[46] K.K. Murray, D.G. Leopold, T.M. Miller, W.C. Lineberger, J. Chem. Phys. 98 (1988) 5442, and references therein.
[47] W. Hack, H.G. Wagner, A. Wilms, Ber. Bunsenges. Phys. Chem. 92 (1988) 620; G. Trinquier, J. Malrieu, J. Am. Chem. Soc. 101 (1979) 7169; L.B. Harding, H.B. Schlegel, R. Krishnan, J.A. Pople, J. Phys. Chem. 84 (1980) 3394.
[48] Z.-X. Wang, R.-Z. Liu, M.-B. Huang, Z. Yu, Can. J. Chem. 74 (1996) 910.

[49] R.J. Berry, D.R.F. Burgess Jr., M.R. Nyden, M.R. Zachariah, C.F. Melius, M. Schwartz, J. Phys. Chem. 100 (1996) 7405.
[50] W.J. Miller, H.B. Palmer, J. Chem. Phys. 40 (1964) 3701.
[51] J.W. Hepburn, D.J. Trevor, J.E. Pollard, D.A. Shirley, Y.T. Lee, J. Chem. Phys. 76 (1982) 4287.
[52] S.G. Lias, Z. Karpas, J.F. Liebman, J. Am. Chem. Soc. 107 (1985) 6089.
[53] C.F. Rodriquez, A.C. Hopkinson, J. Phys. Chem. 97 (1993) 849.
[54] C.F. Rodriquez, D.K. Bohme, A.C. Hopkinson, J. Phys. Chem. 100 (1996) 2942.
[55] W.J. Hehre, L. Radom, P.v.R. Schleyer, J.A. Pople, Ab Initio Molecular Orbital Theory, Wiley, New York, 1986, Chap. 7.
[56] N.G. Rondan, K.N. Houk, R.A. Moss, J. Am. Chem. Soc. 102 (1980) 1770.
[57] F.G. Bordwell, X.-M. Zhang, Acc. Chem. Res. 26 (1993) 510.
[58] C.R. Kemnitz, W.L. Karney, W.T. Borden, J. Am. Chem. Soc. 120 (1998) 3499.
[59] L.V. Gurvich, I.V. Veyts, C.B. Alcock, in Thermodynamic Properties of Individual Substances, Vol. 2, Parts 1 and 2, Hemisphere, New York, 1991.
[60] R.K. Lengel, R.N. Zare, J. Am. Chem. Soc. 100 (1978) 7495; D. Feldman, K. Meier, H. Zacharias, K.H. Welge, Chem. Phys. Lett. 59 (1978) 171; C.C. Hayden, D.M. Neumark, K. Shabatake, R.K. Sparks, Y.T. Lee, J. Chem. Phys. 76 (1982) 3607.
[61] J.L. Holmes, F.P. Lossing, J. Am. Chem. Soc. 110 (1988) 7343.